High and dry: high elevations disproportionately exposed to regional climate change in Mediterranean-climate landscapes

Ian M. McCullough*
Bren School of Environmental Science and Management, 2400 Bren Hall, University of California, Santa Barbara, CA 93106, USA

Frank W. Davis
Bren School of Environmental Science and Management, 2400 Bren Hall, University of California, Santa Barbara, CA 93106, USA

John R. Dingman
Air Resources Board, California Environmental Protection Agency, 10001 I St., P.O. Box 2815, Sacramento, CA 95812, USA

Lorraine E. Flint
U.S. Geological Survey, California Water Science Center, Placer Hall, 6000 J. St., Sacramento, CA 95189, USA

Alan L. Flint
U.S. Geological Survey, California Water Science Center, Placer Hall, 6000 J. St., Sacramento, CA 95189, USA

Josep M. Serra-Diaz
Harvard Forest, Harvard University, Petersham, MA 01366, USA

Alexandra D. Syphard
Conservation Biology Institute, 10423 Sierra Vista Ave, La Mesa, CA 91941, USA

Max A. Moritz
Department of Environmental Science, Policy and Management, 130 Mulford Hall, University of California, Berkeley, CA 94720, USA

Lee Hannah
Betty and Gordon Moore Center for Science and Oceans, Conservation International, 2011 Crystal Drive Suite 500, Arlington, VA 22202, USA

Janet Franklin
School of Geographical Sciences and Urban Planning, Arizona State University, P.O. Box 875302, Tempe, AZ 85287-5302, USA

*corresponding author: Phone: 805-893-7044. Email: imccullough@bren.ucsb.edu.
Draft Submission Date:

Word Count: 5041. Manuscript date: September 1, 2015

Abstract

Context

Predicting climate-driven species' range shifts depend substantially on species' exposure to climate change. Mountain landscapes contain a wide range of topoclimates and soil

5   characteristics that are thought to mediate range shifts and buffer species' exposure. Quantifying fine-scale patterns of exposure across mountainous terrain is a key step in understanding vulnerability of species to regional climate change.

Objectives

We demonstrated a transferable, flexible approach for mapping climate change exposure in a

10   moisture-limited, mountainous California landscape across 4 climate change projections under phase 5 of the Coupled Model Intercomparison Project (CMIP5) for mid-(2040-2069) and end-of-century (2070-2099).

Methods

We produced a 149-year dataset (1951-2099) of modeled climatic water deficit (CWD), which is

15   strongly associated with plant distributions, at 30-m resolution to map climate change exposure in the Tehachapi Mountains, California, USA. We defined climate change exposure in terms of departure from the 1951-1980 mean and historical range of variability in CWD in individual years and three-year moving windows.

Results

20   Climate change exposure was generally greatest at high elevations across all future projections,

though we encountered moderate topographic buffering on poleward-facing slopes. Historically

dry lowlands demonstrated the least exposure to climate change.

Conclusions

In moisture-limited, Mediterranean-climate landscapes, high elevations may experience the

25   greatest exposure to climate change in the 21st Century. High elevation species may thus be

especially vulnerable to continued climate change as habitats shrink and historically energy-

limited locations become increasingly moisture-limited in the future.

Keywords: climate change, microenvironments, range shifts, biogeography, climatic water

deficit, exposure, Mediterranean ecosystems, microrefugia, topographic buffering

30   **Introduction**

         Biogeographers and landscape ecologists are increasingly focusing attention on the role

of local topoclimates and microclimates (hereafter referred to as "microenvironments") in

mediating species' extinction risks and range shifts in response to climate change (Potter et al

2013; Hannah et al 2014). Mountainous topography encompasses a wide variety of

35   microenvironments that may buffer species' exposure to climate change, allowing local retention

or redistribution of species by reducing climate change velocities and providing stepping-stone

habitat connectivity (Loarie et al 2009; Ackerly et al 2010; Scherrer and Korner 2011; De Frenne

et al 2013; Lenoir et al 2013; Hannah et al 2014); both of these factors may be particularly

important for slowly dispersing species (Schloss et al 2012; Zhu et al 2012; Corlett and Westcott

40   2013). Methods are being developed to identify and map the distribution of microenvironments

across landscapes (Ashcroft et al 2012; Dingman et al 2013), with the goal of using this fine-

scale information to improve species distribution models (SDMs) (Franklin et al 2013) and conservation planning under climate change (Anderson et al 2014, Keppel et al. 2015).

45   The vulnerability of species to climate change is a product of their exposure and sensitivity (Williams et al 2008). Although sensitivity is species-specific, climate exposure (hereafter, "exposure") is largely a function of local climate and can thus be projected into the future using downscaled outputs from general circulation models (GCMs). Spatial variation in the magnitude and pace of exposure can be attributed to fine-scale variation in surface energy balance, hydrology, soil characteristics and vegetation structure, all of which are thought to

50   produce *microrefugia*, which are often defined as regionally unique microenvironments that support isolated populations of species outside their main distributions (Rull 2009; Dobrowski 2011). Microrefugia is a term taken from paleoecology, where it is primarily used to describe survival of species through glacial cycles (Bennett et al 1991; Tzedakis et al 2002; McLachlan et al 2005; Stewart et al 2010; Gavin et al 2014; Patsiou et al 2014). Whether the concept is useful

55   in the context of species vulnerability to modern climate change is a topic of ongoing research and discussion (Hannah et al 2014). For isolated populations to persist through periods of rapid climate change, the microenvironments they inhabit must be somewhat climatically decoupled from regional climate for those climate factors that limit the species' distribution (Dobrowski 2011; Hylander et al 2015).

60   Conceptually, climate change at a given site constitutes a change in the probability distributions of climate variables with associated changes in descriptors of those distributions (e.g., the mean and standard deviation of the normal distribution) (Katz and Brown 1992). Changes in extremes can be particularly influential in natural systems (Easterling et al 2000) and may be masked by analyses focused on changes in long-term means (Polade et al 2014). Here we

65   present an approach for quantifying the magnitude of exposure at a given site along two main

axes representing change in mean annual climate and in frequency of climate extremes relative to

the historical range of variability (HRV, Landres et al 1999; Maher et al in review) in a historical

reference period (Fig. 1). Exposure has been broadly defined as encompassing both the rate and

magnitude of climate change (Dawson et al 2011) and combined changes in both mean climate

70   and frequency of extreme events have been previously used to assess exposure (Williams et al

2007; Beaumont et al 2011; Benito-Garzon et al. 2014). In mountainous regions we would

expect sites to vary considerably in the rate of change in both means and extremes relative to the

regional trend. Ignoring dispersal limitations, microrefugia would arguably be associated with

those sites that show the least change from historical conditions (i.e., fall as near to the origin of

75   these two axes as possible) and are thus least coupled to regional climate trends. Vulnerability of

individual species will ultimately depend on their sensitivity to changes in mean and/or extreme

conditions.

#Figure 1 approximately here#

We applied our approach and concept of exposure to a biologically diverse mountainous

80   study region in southern California. Because we were especially interested in plant distributions,

we modeled and analyzed fine-scale changes in climatic water deficit (CWD), a bioclimatic

variable that exerts strong, topographically-driven controls on plant distributions in

Mediterranean-climate landscapes of California and elsewhere (Stephenson 1998; Lutz et al

2010). We focused solely on CWD because it integrates interactions among temperature,

85   precipitation and soil properties, all of which play a strong role in determining species

distributions. Our research questions were: 1) How is CWD projected to change across a rugged

landscape under mid-century and end-of-century climate projections in comparison to historical

conditions? 2) How will rates of climate change exposure vary across the landscape as a function of local microenvironments?

Methods

Study Area

Our study area was located in the western Tehachapi Mountains, California, USA (34°58′N, 118°35′W). This area, which is the site of ongoing research to measure and model microclimates and plant establishment (Davis and Sweet 2012), is characterized by rugged topography and steep climate gradients, providing a suitable case study of local variation in climate and projected climate change exposure. The area is mostly private land owned and managed by the Tejon Ranch Company for cattle ranching, hunting, agriculture and rare species conservation. Our climate grids and study area covered a rectangular subregion of Tejon Ranch and some adjacent areas to the northeast, spanning approximately 33,000 ha and steep elevational gradients (370-2,364 m) (Fig. 2). The climate is Mediterranean, with hot, dry summers and cool, wet winters. Mean annual precipitation for the period 1896-2010 varied from around 250 mm in the driest, low elevation portions of the area to over 500 mm at the highest elevations. At elevations above roughly 1500-1600 m, precipitation regimes are historically snow-dominated (Western Regional Climate Center 2015). Our focal climate indicator (CWD) varies widely across the landscape, mainly as a result of topographically controlled variation in solar radiation, temperature and precipitation but also due to differences in soil water holding capacity (Fig. 3). At low elevations, soils are granite-derived, coarse-loamy thermic typic Haploxerolls with maximum depths of approximately 61-122 cm (USDA 2015). High elevation sites include coarse-sandy loams derived from schist and classified as mesic Pachic

110 Haploxerolls, as well as granite-derived medium- and coarse-sandy loams classified as mesic

Haploxerolls. Maximum soil depths at high elevations are approximately 127-229 cm (USDA

2015). The topographically varied landscape supports diverse vegetation cover ranging from arid

grasslands and shrublands to deciduous and evergreen oak woodlands and montane conifer

forests.

115 #Figure 2 approximately here#

#Figure 3 approximately here#

#Table 1 approximately here#

Mapping historical and projected future climates

To represent historical climate conditions, PRISM (Parameter-elevation Relationships

120 on Independent Slopes Model) (Daly et al 2008) temperature and precipitation data were

spatially downscaled from 800 to 30 m using Gradient-Inverse-Distance-Squared (GIDS)

downscaling (Flint and Flint 2012). This method basically drapes the downscaled climate data

over the landscape and has been shown either to match the coarser resolution gridded climate or

improve the match to measured station data for both precipitation and air temperature by

125 incorporating local topography, adiabatic lapse rates and climatic gradients (Flint and Flint

2012). A validation exercise was performed to provide evidence of the local skill in the

downscaling for our site by comparing downscaled climate to weather station data collected at

our study sites for 2012-2013 that were not used in downscaling. Correlation (r) of observed with

modeled monthly averages of daily maximum air temperatures in 2013 was 0.99 (Mean Absolute

130 Error (MAE) = 1.73 °C) for foothill stations and 0.95 (MAE = 1.66°C for montane stations.

Correlation for minimum air temperatures was 0.97 (MAE = 1.51 °C) and 0.97 (MAE = 1.97 °C)

for foothill and montane stations (3 of each), respectively, in 2013. Very similar results were obtained for 2012. Interpolated precipitation values were not as reliable. At foothill stations, correlation with monthly precipitation was 0.85 (MAE = 16 mm) in 2012 and 0.77 (MAE = 14.4 mm) in 2013. At montane stations, correlation was 0.94 (MAE = 6 mm) in 2012 and 0.84 (MAE = 6 mm) in 2013.

We analyzed 4 future projections that bracketed a reasonable range of climate futures for the Tehachapi landscape (Table 1). Due to computational constraints, we downscaled a strategic subset of Coupled Model Intercomparison Project Phase 5 (CMIP5) climate projections as part of our larger study (Davis and Sweet 2012). We chose projections using a clustering analysis that plotted future projections along two axes and directions of climate change (temperature and precipitation), placing projections in one of four quadrants (hot-dry, cool-dry, hot-wet and cool-wet) for our study area (Weiss et al in review). We then reduced this set to nine projections that bracketed the range of climate projections across the four quadrants, which included three RCP 8.5, one RCP 6.0, two RCP 4.5 and three RCP 2.6 projections. For our study, we only considered RCP 8.5 (business-as-usual emissions for the 21st Century) and 4.5 (stabilizing emissions by mid-21st Century) because 1) RCP 6.0 futures are bracketed by RCP 8.5 and 4.5 projections and 2) RCP 2.6 projections are overly optimistic relative to current emissions trajectories in their requirement for declining rather than stabilizing radiative forcing by 2100 (Van Vuuren et al 2007). The RCP 4.5 subset included the Model for Interdisciplinary Research on Climate (MIROC) and the Max Planck Institute Earth System Model (MPI). We reduced the three RCP 8.5 model subset to the Community Climate System Model v4 (CCSM4) and MIROC, excluding the intermediate model, the Flexible Global Ocean-Atmosphere-Land System Model (FGOALS), in order to use an equal number of RCP 8.5 and 4.5 projections in this study. We did not consider

155 projections of negative temperature change due to their unrealistic nature, so we instead selected

projections that were relatively cooler than the RCP 8.5 projections. We calculated the average

changes projected for our study area using each model (Table 1) to verify that local projections

for Tejon Ranch covered our four target climate scenarios (hot-dry, cool-dry, hot-wet and cool-

wet).

160 Future projections were downscaled using the method of constructed analogues with

bias correction and GIDS interpolation (Flint and Flint 2012). In our study area, downscaled

CCSM4 and MPI models project relatively small increases in precipitation when comparing

1951-1980 to end-of-21st-century (2070-2099) levels, whereas MIROC predicts considerable

decreases over the same time frame (Flint and Flint 2014). Air temperatures are projected to

165 increase ~1.9 to 4.6°C across the four models (Table 1). We acknowledge, however, that these

30-year mean climate descriptions potentially mask changes in temporal frequency of weather

events, particularly prolonged droughts and large storms (Polade et al 2014, Berg and Hall

2015).

Modeling CWD

170 Mapping exposure requires accurate representation of microenvironments at biologically

appropriate scales (Franklin et al 2013; Potter et al 2013). We produced a 149-year (1951-2099),

30-m spatial resolution dataset of annual water-year (Oct 1-Sep 30) accumulated climatic water

deficit (CWD) using the Basin Characterization Model (BCM). The BCM is a distributed-

parameter, deterministic water balance model used to estimate potential recharge on a monthly

175 time step (Flint et al 2004, 2013). The model accounted for variation in climatic and edaphic

conditions, integrating spatial data on precipitation amount, timing and storage, minimum and

maximum air temperature, relative humidity, radiation (net short and longwave), soil-water

holding capacity and vegetative cover. The BCM was calibrated and validated with 68 and 91

California watersheds, respectively, to ensure the model was regionally robust (Flint et al 2013).

180   Soil information was obtained from SSURGO soil databases (NRCS 2006). These climate grids

were spatially downscaled using GIDS methodology applied to local elevational gradients in a

multi-step process from 12 to 4 km to 30 m (Flint and Flint 2012). Potential and actual

evapotranspiration were calculated using the Priestley and Taylor (1972) equation and the

National Weather Service Snow-17 model (Anderson 1976). Amounts of available water below

185   field capacity were considered as actual evapotranspiration (Flint et al 2013). CWD was

calculated as the difference between potential and actual evapotranspiration. CWD integrates

precipitation, energy loading, soil water storage, and evapotranspiration and corresponds to water

that would be used by plants if it were available, and relates well to the distribution of dominant

plant species (Stephenson 1998). Because CWD relies heavily on temperature-induced increases

190   in PET, CWD increases in nearly all future climate projections (Supp. Fig. 1).

Analyzing projected changes in CWD and mapping climate change exposure

To characterize the historical reference climate, we calculated mean annual accumulated

water-year CWD (CWD_{WY}) for the period 1951-1980 for each 30-m grid cell (Fig. 3). We use

the period of 1951-1980 as our historical baseline due to relatively stationary temperatures prior

195   to rapid global warming in the 1980s (Fig.1 in Hansen et al 2006). CWD_{WY} showed no

significant directional trend in our study area during this period. Prior to 1951 we lacked

sufficient station data for reliable modeling of CWD across the region.

We analyze departure from historical mean conditions (ΔCWD_{WY}) and frequency of extreme years (ΔHRV) for each 30-m cell (368,520 cells) at mid-(2040-2069) and end-of-century (2070-2099) for each CMIP5 projection. Mean CWD_{WY} increased everywhere in the landscape over the course of the 21st Century, so departure from baseline mean CWD_{WY} measures the relative shift towards drier conditions of each cell. Our approach to identifying changes in extreme years was somewhat similar to that of Klausmeyer et al (2011), who analyzed HRV in climate variables to define a "coping range" vs. stressful climate conditions for landscapes in California. We used the frequency distribution of annual CWD values within the historical reference period to define climatic extremes for each grid cell in the landscape. We expressed the departure as a percentage rather than absolute change given the more than 3-fold range in average CWD_{WY} across the region. We defined departure from the historical range of variability (HRV) in drought years as the number of years in each 30-year period in which CWD_{WY} exceeded approximately the 93rd percentile of the HRV (i.e., drier than all but the 2 driest years in the reference period) for each cell. We did not consider variation in extremely wet years relative to historical conditions. Because the 93% threshold is somewhat arbitrary, we tested the sensitivity of results to cutoffs at approximately the 90th and 87th percentiles. To evaluate changes in the likelihood of multi-year droughts, which may be especially stressful to long-lived plants (Bigler et al 2007; Vicente-Serrano et al 2013), we also analyzed historical departure in three-year moving windows ($\Delta HRV3$) for the same set of GCMs, time periods and HRV thresholds. Analyses were performed using the R package "raster" (Hijmans 2015).

Arguably, sites with minimal divergence from historical climate in terms of changes in mean climate and frequency of extreme years (years outside the HRV) offer the greatest potential as microrefugia (Fig. 1). As shown in Fig. 1, the distance of a site from the origin in this two-

dimensional space represents climate exposure, which we labeled an exposure score. To facilitate comparison to percent change from mean historical climate, we re-scaled the frequency of extreme years from 0-30 to 0-100. Although previous studies used combinations of both mean climate change and frequency of extreme events to assess climate change exposure, methods

225   varied somewhat in terms of temporal scaling and relative contributions of means vs. extremes. As such, we calculated climate change exposure as $(\Delta CWD_{WY}^2 + \Delta HRV^2)^{0.5}$, providing equal weight to changes in mean vs. extreme climate. We mapped exposure scores across the landscape for each future projection, focusing on end-of-century projections to emphasize the requisite long-term climatic decoupling of microrefugia.

230   **Results**

Climatic water deficit

Spatial patterns of ΔHRV were similar across climate projections and time periods, but varied in magnitude (Figs. 4 and 5, Table 2). Projected ΔCWD_{WY} changes in both means (Supp. Figs. 2-3) and ΔHRV increased with elevation and were highest on equator-facing slopes. Under

235   the warmest and driest projection (MIROC RCP 8.5), ΔHRV ranged from 11 to 30 out of 30 years (Fig. 4) and ΔCWD_{WY} increased 13-67% by end-of-century (Supp. Fig. 2). Mitigated emissions projections (RCP 4.5) showed less divergence from the HRV and historical mean climate, particularly under the wetter MPI model (Supp. Fig. 3). Lowering the HRV thresholds slightly increased ΔHRV, particularly maximum values in RCP 4.5 projections (Table 2). Cells

240   with the lowest ΔHRV departure rates were less sensitive to changes in thresholds across all projections (Table 2).

Values of ΔHRV3 were generally similar to ΔHRV, but with lower maxima (Table 3). Spatial patterns across the landscape were also similar, with the greatest departure rates at high elevations and lower rates on poleward (north)-facing slopes than equator-facing slopes at the

245   same elevations. Contrary to the single-year analysis, however, rates of three-year departures from historical climate were insensitive to more restrictive definition of the HRV (Table 3).

#Table 2 approximately here#

#Table 3 approximately here#

#Figure 4 approximately here#

250   #Figure 5 approximately here#

Mapping climate change exposure

Across all projections, exposure scores generally increased with elevation (Fig. 6, Supp. Fig. 4). However, exposure scores varied widely across the landscape and across projections, ranging from 17 for some locations under MPI to a maximum of 119 under MIROC RCP 8.5.

255   Scatterplots of ΔCWD_{WY} versus ΔHRV (cf. Fig 1) for each projection at end-of-century indicated that high exposure scores mainly result from high ΔHRV (Fig. 6). Topographic buffering of climate exposure occurs on poleward-facing slopes, but these areas still received relatively high exposure scores compared to flat lowlands, particularly those below 500 m (Fig. 6). Because complex topography somewhat obscures the buffering effects of poleward-facing

260   slopes, we performed a post hoc regression tree analysis (RTA) using the R package "tree" (Ripley 2015) to explore relationships among exposure, elevation and northness (calculated as

sin(slope) * cos(aspect)). The RTA revealed that although elevation was the primary control on exposure, northness reduced exposure at moderate and low elevations (Supp. Fig. 5).

#Fig. 6 approximately here#

265

Discussion

Spatial patterns of climate change exposure

Large variation in CWD-based climate exposure scores suggests considerable decoupling of local sites from regional climate trends in mountain landscapes. Whether this decoupling is

270   adequate to support microrefugia ultimately depends on widely varying species' sensitivity to changes in either or both ΔCWD_{WY} and ΔHRV. The lowest exposure scores in our landscape occurred at low elevations in sites that currently experience high CWD_{WY} and will continue to do so throughout the 21st Century. Plant species currently occupying these sites (mainly annual grasses and forbs) tolerate dry conditions, though this is not to say these species are not

275   vulnerable to other dimensions of climate change. For example, grasslands are sensitive to the timing as well as the amount of soil moisture (Hobbs et al 2007).

We might expect microrefugia to occur in the highest (cooler and moister) portions of mountain landscapes. Our analysis suggests the opposite could be true. Those sites with historically low CWD_{WY} levels have the potential for relatively larger increases in ΔCWD_{WY}

280   associated with warming that can affect actual evapotranspiration (AET) (Stephenson 1998). This will be especially true for historically snow-dominated sites that will receive an increasing fraction of precipitation as rain as well as shorter snowpack duration with associated increases in

runoff, AET and soil evaporation (Rangwala and Miller 2012; Rangwala et al 2013). Depending

on water availability, AET will increase initially in response to warming temperatures, but will

285   eventually level off and decline when available water is exhausted (Rosenberg et al 1983).

Exhaustion of water supplies can lead to plant mortality and vegetation type conversions

(Breshears et al 2005). Consequently, plant communities currently found at the highest

elevations in moisture-limited landscapes may face shrinking habitat and limited opportunities

for long-term survival under accelerated climate exposure (Gottfried et al 2012).

290   Changes in water availability coincident with increasing temperatures at high elevations

are consistent with projections for our study area. In our study region, departure from historical

CWD regimes was particularly dramatic at elevations above approximately 1700 m (Figs 4-5).

This elevation currently marked a shift from snow-dominated to rain-dominated precipitation. By

end-of-century, winter temperatures are projected to raise the rain-snow transition zone above

295   approximately 1700 m in the RCP 4.5 scenarios and above 2000 m in CCSM4 RCP 8.5, and

convert the entire landscape to rain-dominated under MIROC RCP 8.5. At lower elevations,

snow was historically less important or absent entirely, so changes in moisture availability in

these locations are projected to be a function of changes in total precipitation. Therefore, we

suspect that sites historically within the rain-snow transition zone in moisture-limited landscapes

300   may be most exposed to climate change. Although absent from our landscape, locations that are

strongly temperature-limited and that are currently far from the rain-snow transition zone (e.g.,

alpine or subalpine habitats) are unlikely to experience departures from historical climate as

dramatic as those projected at Tejon Ranch. More generally, we would expect that both changes

in overall precipitation and the position of the rain-snow transition zone will combine to

305   influence the exposure of any given site (Tague and Peng 2013; Thorne et al 2015).

Although high elevation areas within the changing rain-snow transition zone are likely to become increasingly "high and dry", we observed some buffering of these effects on poleward-facing slopes, which may be less exposed to climate change than other aspects and ridgetops. Systematically lower solar irradiance, lower potential evapotranspiration and longer snowpack duration compared to the rest of the landscape combined to reduce the local rate of departure from historical climate. Buffering of losses in snowpack on poleward-facing slopes may be particularly important for snow-dependent species (Curtis et al 2014). The RTA revealed that exposure was primarily controlled by elevation in our study landscape, but with secondary, interactive effects of northness (Supp. Fig. 5). On the highest poleward-facing slopes (Fig. 6), exposure was particularly great due to warming-induced loss of historically important snow. Snow reduction accelerated increases in CWD and negated topographic buffering of northerly aspects. At lower elevations, where snow was historically uncommon or absent, poleward-facing slopes exhibited some buffering of exposure. Conversely, vegetation density and local land management history may combine to increase AET in some cases and negate the additional moisture availability on poleward-facing slopes (Guarin and Taylor 2005). Finally, absent from our discussion have been riparian areas, which were not directly defined by the BCM because, although this model calculated recharge, it did not incorporate lateral flow. Riparian areas may also reduce climate change exposure due to accumulation of moisture, cool air and shade-providing vegetation. These topographically derived distinctions in climatic conditions represent a form of decoupling from regional climate and may produce potential microrefugia.

On the transferability of our approach

The approach we described here using departure from historical climate as a method of examining climate change exposure across landscapes is widely transferrable to other

landscapes, useful for conservation planning and not subject to arbitrary decisions on the spatial

330   extent of analysis. Although transferability will be ultimately limited by spatial (and possibly

temporal) resolution of climate grids, fine spatial resolution is essential for identifying

microenvironments and potential microrefugia. Increasingly fine spatial resolution has been

shown to reduce rates of range shifts owing to better detection of microenvironments (Serra-Diaz

et al 2014). We recognize that downscaling from coarse GCM grids to local topoclimates

335   introduces additional uncertainty into climate projections that remains poorly quantified (Hall

2014), but nevertheless downscaled climate projections are useful for the purpose of ecological

vulnerability assessment (Franklin et al 2013). Use of varying time windows (e.g., ΔHRV vs.

ΔHRV3) provides additional flexibility in terms of temporal scaling of the interactions among

climate change and species' tolerance limits. Definitions of the HRV may also be manipulated

340   depending on the nature of the distribution of focal climate variables across years. Because our

method is not tied to specific biological targets, it allows local managers to decide how local

changes in climate variables interact with biological sensitivity and translate into changes in

species distributions. Managers could group cells of similar rates of historical departure (e.g., 0-5

of 30 years) to analyze patch structure and configuration, if desired. In these more specific

345   contexts, it may make sense to view landscapes through the lens of individual species (e.g.,

commercially valuable or keystone species); however, we believe that the generic nature of our

approach boosts its transferability.

Conclusions

    Considering that a common, stated objective in conservation is to protect species in the

350   places they currently inhabit, in regions undergoing rapid climate change, microrefugia should be

sites that protect the same species both now and in the future. In this vein, the allure of

microrefugia is understandable. If we could only identify parts of landscapes somehow immune

or resistant to climate change, we could protect and/or actively manage these sites to prevent

extinctions (Keppel et al 2012). Our analyses, however, suggest that such sites may be limited to

355   rare localities in future landscapes. Nonetheless, we illustrate how the magnitude of climate

change exposure can vary widely over short distances in heterogeneous topography and provide

a means for locating areas that could experience less climate change and lower change velocities

relative to regional trends. These areas may be especially valuable conservation and management

targets and may play important roles in mediating range shifts and/or local persistence of species

360   (Hannah et al 2014, Serra-Diaz et al 2015).

370

References

Ackerly DD, Loarie SR, Cornwell WK, Weiss SB, Hamilton H, Branciforte R, Kraft NJB (2010)
The geography of climate change: implications for conservation biogeography. Divers Distrib
16:476-487

375

Anderson EA (1976) A point energy and mass balance model of a snow cover. Technical report NWS 19, 150 p. U.S National Oceanographic and Atmospheric Administration (NOAA). Silver Spring, MD.

380   Anderson MG, Clark M, Sheldon AO (2014) Estimating Climate Resilience for Conservation across Geophysical Settings. Conserv Biol 28:959-970

Ashcroft MB, Gollan JR, Warton DI, Ramp D (2012) A novel approach to quantify and locate potential microrefugia using topoclimate, climate stability, and isolation from the matrix. Glob
385   Chang Biol 18:1866-1879

Beaumont LJ, Pitman A, Perkins S (2011) Impacts of climate change on the world's most exceptional ecoregions. Proc Natl Acad Sci 108:2306-2311

390   Benito-Garzon M, Leadley PW, Fernandez-Manjarres JF (2014) Assessing global biome exposure to climate change through the Holocene-Anthropocene transition. Glob Ecol Biogeogr 23:235-244.

Bennett KD, Tzedakis, PC, Willis, KJ (1991) Quaternary refugia of north European trees. J
395   Biogeogr 18:103-115

Berg N, Hall, A (2015) Increased interannual precipitation extremes over California under climate Change. J Climate 28:6324-6334.

400   Bigler C, Gavin DG, Gunning C, Veblen TT (2007) Drought induces lagged tree mortality in a subalpine forest in the Rocky Mountains. Oikos 116:1983-1994

Breshears DD, Cobb NS, Rich PM et al (2005) Regional vegetation die-off in response to global-change-type drought. P Natl Acad Sci USA 102:15144-15148
405
Corlett RT, Westcott DA (2013) Will plant movements keep up with climate change? Trends Ecol Evol 28:482-488

Curtis JA, Flint LE, Flint AL, Lundquist JD, Hudgens B, Boydston EE, Young JK (2014)
410   Incorporating Cold-air pooling into downscaled climate models increases potential refugia for snow-dependent species within the Sierra Nevada Ecoregion, CA. *PLoS One*. doi: 10.1371/journal.pone.0106984

Daly C, Halbleib M, Smith JI, Gibson WP, Dogget MK, Taylor GH, Pasteris PP (2008)
415   Physiographically sensitive mapping of climatological temperature and precipitation across the conterminous United States. Int J Climatol 28 doi: 10.1002/joc

Davis FW, Sweet LC. From mountain microclimates to the macroecology of tree species distributions in California. Mountain Views 6:2-5.
420

Dawson TP, Jackson ST, House JI, Prentice IC, Mace GM (2011). Beyond predictions: biodiversity conservation in a changing climate. Science 332: 53-58

De Frenne P, Rodríguez-Sánchez F, Coomes DA et al (2013) Microclimate moderates plant responses to macroclimate warming. P Natl Acad Sci USA 110: 18561-18565

Dingman JR, Sweet LC, McCullough I, Davis FW, Flint A, Franklin J, Flint LE (2013) Cross-scale modeling of surface temperature and tree seedling establishment in mountain landscapes. Ecol Process 2: 1-15

Dobrowski SZ (2011) A climatic basis for microrefugia: the influence of terrain on climate. Global Chang Biol 17: 1022-1035

Easterling DR, Meehl GA, Parmesan C, Changnon SA, Karl TR, Mearns LO (2000) Climate Extremes: Observations, Modeling, and Impacts. Science 289:2068–2074

Flint LE, Flint AL (2014) California Basin Characteristic Model: a dataset of historical and future hydrologic response to climate change: U.S. Geological Survey data release. doi:10.5066/F76T0JPB.

Flint LE, Flint AL (2012) Downscaling future climate scenarios to fine scales for hydrologic and ecological modeling and analysis. Ecol Process 1:1-15

Flint LE, Flint AL, Thorne JH, Boynton R (2013) Fine-scale hydrologic modeling for regional landscape applications: the California Basin Characterization Model development and performance. Ecol Process 2:1-21.

Flint AL, Flint LE, Hevesi JA, Blainey JB (2004) Fundamental Concepts of Recharge in the Desert Southwest: A Regional Modeling Perspective, in Groundwater Recharge in a Desert Environment: The Southwestern United States (eds J. F. Hogan, F. M. Phillips and B. R. Scanlon), American Geophysical Union, Washington, D. C.. doi: 10.1029/009WSA10

Franklin J, Davis FW, Ikegami M, Syphard AD, Flint LE, Flint AL, Hannah L (2013) Modeling plant species distributions under future climates: how fine scale do climate projections need to be?. Glob Chang Biol 19:473-483

Gavin DG, Fitzpatrick MC, Gugger PF, Heath KD, Rodríguez-Sánchez F, Dobrowski SZ., ... & Williams, J. W. (2014). Climate refugia: joint inference from fossil records, species distribution models and phylogeography. New Phyto 204:37-54

Gottfried M, Pauli H, Futschik A et al (2012) Continent-wide response of mountain vegetation to climate change. Nature Clim Change 2:111-115

Guarín A, Taylor AH (2005) Drought triggered tree mortality in mixed conifer forests in Yosemite National Park, California, USA. Forest Ecol and Manag 218:229-244

Hannah L, Flint L, Syphard AD, Moritz MA, Buckley LB, McCullough IM (2014) Fine-grain modeling of species' response to climate change: holdouts, stepping-stones, and microrefugia. Trends Ecol Evol 29:390-397

470

Hansen J, Sato M, Ruedy R, Lo K, Lea DW, Medina-Elizade M (2006) Global temperature change. P Natl Acad Sci USA 103:14288-14293

Hijmans RJ (2015) raster: Geographic data analysis and modeling. R package version 2.3-33.
475   http://CRAN.R-project/org/package=raster

Hobbs RJ, Yates S, Mooney HA (2007) Long-term data reveal complex dynamics in grassland in relation to climate and disturbance. Ecol Mongr 77:545-568.

480   Hylander K, Ehrlén J, Luoto M, Meineri E (2015) Microrefugia: Not for everyone. Ambio 44:60-68.

Katz R, Brown B (1992) Extreme events in a changing climate: Variability is more important than averages. Climatic Change 21:289–302

485

Keppel G, Mokany K, Wardell-Johnson GW, Phillips BL, Welbergen J, Reside AE (2015) The capacity of refugia for conservation planning under climate change. Front Ecol Environ 13:106-112.

490   Keppel G, Van Niel KP, Wardell-Johnson GW, Yates CJ, Byrne M, Mucina L, Schut AGT, Hopper SD, Franklin SE (2012) Refugia: identifying and understanding safe havens for biodiversity under climate change.

Klausmeyer KR, Shaw MR, MacKenzie JB, Cameron DR (2011) Landscape-scale indicators of
495   biodiversity's vulnerability to climate change. Ecosphere 2:art 88.
http://dx.doi.org/10.1890/ES11-00044.1

Landres PB, Morgan P, Swanson FJ (1999) Overview of the use of natural variability concepts in managing ecological systems Ecol Appl 9:1179-1188.

500

Lenoir J, Graae BJ, Aarrestad PA et al (2013) Local temperatures inferred from plant communities suggest strong spatial buffering of climate warming across Northern Europe. Glob Chang Biol 19:1470-1481

505   Loarie SR, Duffy PB, Hamilton H, Asner GP, Field CB, Ackerly DD (2009) The velocity of climate change. Nature 462:1052-1055.

Lutz JA, van Wagtendonk JW, Franklin JF (2010) Climatic water deficit, tree species ranges, and climate change in Yosemite National Park. J Biogeogr 37:936-950.

510

Maher SP, Morelli TL, Hershey M, Flint AL, Flint LE, Moritz C, Beissinger SR (in review) Erosion of refugia in the Sierra Nevada meadows network with climate change.

McLachlan JS, Clark JS, Manos PS (2005) Molecular indicators of tree migration capacity under rapid climate change. Ecology 86:2088-2098

Moritz MA, Parisien MA, Batllori E, Krawchuk MA, Van Dorn J, Ganz DJ, Hayhoe K (2012) Climate change and disruptions to global fire activity. Ecosphere 3:1-22.

NRCS (2006) Natural Resources Conservation Service: U.S. General Soil Map (SSURGO/STATSGO2). http://www.ftw.nrcs.usda.gov/stat_data.html, http://soils.usda.gov/survey/geography/statsgo/description.html

Patsiou TS, Conti E, Zimmermann NE, Theodoridis S, Randin CF (2014) Topo-climatic microrefugia explain the persistence of a rare endemic plant in the Alps during the last 21 millennia. Glob Chang Biol 20:2286-2300

Polade SD, Pierce DW, Cayan DR, Gershunov A, Dettinger MD (2014) The key role of dry days in changing regional climate and precipitation regimes. Sci Rep 4:4364.

Potter KA, Arthur Woods H, Pincebourde S (2013) Microclimatic challenges in global change biology. Glob Chang Biol 19:2932-2939

Priestley CHB, Taylor RJ (1972) On the assessment of surface heat flux and evaporation using large-scale parameters. Monthly Weather Rev 100:81–92

Rangwala I, Miller JR (2012) Climate change in mountains: a review of elevation-dependent warming and its possible causes. Clim Change 114:527-547

Rangwala I, Sinsky E, Miller JR (2013) Amplified warming projections for high altitude regions of the northern hemisphere mid-latitudes from CMIP5 models. Environ Res Lett. Doi:10.1088/1748-9326/8/2/024040

Ripley B (2015) tree: Classification and regression trees. R package version 1.0-36. http://CRAN.R-project.org/package=tree

Rosenberg NJ, Blad BL, Verma SB (1983) Microclimate: The biological environment, Wiley

Rull V (2009) Microrefugia. J Biogeogr 36:481-484

Scherrer D, Körner C (2011) Topographically controlled thermal-habitat differentiation buffers alpine plant diversity against climate warming. J Biogeogr 38:406-416

Schloss CA, Nuñez TA, Lawler JJ (2012) Dispersal will limit ability of mammals to track climate change in the Western Hemisphere. P Natl Acad Sci USA 109:8606-8611

Serra-Diaz JM, Franklin J, Ninyerola M, Davis FW, Syphard AD, Regan HM, Ikegami M. (2014) Bioclimatic velocity: the pace of species exposure to climate change. Divers Distrib 20:169-180

Serra-Diaz JM, Scheller RM, Syphard AD, Franklin J (2015) Disturbance and climate microrefugia mediate tree range shifts during climate change. Landscape Ecology 30:1039–1053

Stephenson N (1998) Actual evapotranspiration and deficit: biologically meaningful correlates of vegetation distribution across spatial scales. J Biogeogr 25:855-870

Stewart JR, Lister AM, Barnes I, Dalén L (2010) Refugia revisited: individualistic responses of species in space and time. P Roy Soc B-Biol Sci 277:661-671

Tague C, Peng H (2013) The sensitivity of forest water use to the timing of precipitation and snowmelt recharge in the California Sierra: Implications for a warming climate. J Geophys Res-Biogeo 118:875-887

Thorne JH, Boynton RM, Flint LE, Flint AL (2015) The magnitude and spatial patterns of future hydrologic change in California's watersheds. Ecosphere 6:art 24.
http://dx.doi.org/10.1890/ES14-00300.1

Tzedakis PC, Lawson IT, Frogley MR, Hewitt GM, Preece RC (2002) Buffered tree population changes in a Quaternary refugium: evolutionary implications. Science 297: 2044-2047

USDA (2015) U.S. Department of Agriculture. https://soilseries.sc.egov.usda.gov/. Accessed 24 Mar 2015.

Van Vuuren DP, Den Elzen MGJ, Lucas PL, Eickhout B, Strengers BJ, Van Ruijven B, Wonink S, Van Houdt R (2007) Stabilizing greenhouse gas concentrations at low levels: an assessment of reduction strategies and costs. Clim Change 81:119-159.

Vicente-Serrano SM, Gouveia C, Camarero JJ et al (2013) Response of vegetation to drought time-scales across global land biomes. P Natl Acad Sci 110:52-57

Western Regional Climate Center (2015) Desert Research Institute. http://www.wrcc.dri.edu/. Accessed 21 Jan 2015

Weiss SB, Flint L, Flint A, Micheli L (in review) Choosing your futures: high resolution climate-hydrology scenarios for San Francisco Bay Area, California.

Williams JW, Jackson ST, Kutzbach JE (2007) Projected distributions of novel and disappearing climates by 2100 AD. Proc Natl Acad Sci 104:5738-5742.

Williams SE, Shoo LP, Isaac JL, Hoffmann AA, Langham G (2008) Towards an integrated framework for assessing the vulnerability of species to climate change PLoS Biol 6:e325

Zhu K, Woodall CW, Clark JS (2012) Failure to migrate: lack of tree range expansion in response to climate change. Glob Chang Biol 18:1042-1052

605

Table 1. CMIP5 models used for analysis and projected climate change between baseline (1951-1980) and end-of-century (2070-2099) at Tejon Ranch. WY = water-year (Oct 1-Sep 30), cwd = climatic water deficit.

GCM	RCP	July tmax (°C)	Jan tmin (°C)	WY precip (mm)	WY cwd (mm)
Max Planck Institute Earth System Model (MPI)	4.5	1.94	1.98	24.38	92.58
Model for Interdisciplinary Research on Climate (MIROC)	4.5	2.6	1.94	-67.64	156.54
Community Climate System Model (CCSM4)	8.5	4.07	4.02	14.87	148.82
Model for Interdisciplinary Research on Climate	8.5	4.63	4.61	-111.2	244.79

610

615

Table 2. Number of years (out of 30) with accumulated water-year climatic water deficit (CWD) outside the historical range of variability (presented as landscape minimum and maximum values)

	93%		90%		87%	
GCM	**Mid**	**End**	**Mid**	**End**	**Mid**	**End**
CCSM4 RCP 8.5	2, 24	5, 29	2, 28	5, 30	2, 28	8, 30
MIROC RCP 8.5	2, 27	11, 30	2, 30	11, 30	2, 30	16, 30
MIROC RCP 4.5	2, 22	6, 27	2, 29	6, 30	2, 29	7, 30
MPI RCP 4.5	1, 19	2, 20	2, 27	2, 24	4, 28	4, 25

620

625

630

Table 3. Number of years (out of 30) with accumulated water-year climatic water deficit (CWD) outside the historical range of variability (presented as minimum and maximum landscape values) using moving 3-year averages

GCM	93%		90%		87%	
	Mid	End	Mid	End	Mid	End
CCSM4 RCP 8.5	1, 23	5, 27	1, 23	5, 27	1, 23	5, 27
MIROC RCP 8.5	2, 28	9, 28	2, 28	9, 28	2, 28	9, 28
MIROC RCP 4.5	2, 22	6, 26	2, 22	6, 26	2, 22	6, 26
MPI RCP 4.5	2, 20	2, 20	2, 20	2, 20	2, 20	2, 20

635

640

Figure Captions

Fig. 1. Conceptual diagram of potential microrefugia in terms of climate change exposure, which is a function of both changes in mean climate and frequency of extremes relative to historical climate. The exposure of a given site is determined by its position along these two main axes.

645 Fig. 2. Study site. Tejon Ranch is located in the Tehachapi Mountains, California, USA, near the southern edge of the San Joaquin Valley and the Sierra Nevada. Our model domain (inset box) covers 33,000 ha and an elevational gradient of 370-2364 m.

Fig. 3. Frequency distribution of accumulated water-year climatic water deficit (CWD) for Tejon Ranch expressed as cell means for 1951-1980.

650 Fig. 4. Number of years of departure from the historical range of variability in terms of accumulated water-year climatic water deficit (mm/yr) during mid- (2040-2069) and end-of-century (2070-2099) periods for two general circulation models (GCMs) at representative concentration pathways of 8.5: the Community Climate System Model v4 (CCSM4) and the Model for Interdisciplinary Research on Climate (MIROC).

655 Fig. 5. Number of years of departure from the historical range of variability in terms of accumulated water-year climatic water deficit (mm/yr) during mid- (2040-2069) and end-of-century (2070-2099) periods across two general circulation models (GCMs) at representative concentration pathways of 4.5: the Model for Interdisciplinary Research on Climate (MIROC) and the Max Planck Institute Earth System Model (MPI).

660 Fig. 6. Relative climate change exposure across all four climate change projections at end-of-century (2070-2099). Exposure scores were calculated for each future projection as the product of the percent change in mean climate and the rate of extreme years (departures from the HRV). Presented here are mean exposure scores across all four projections.
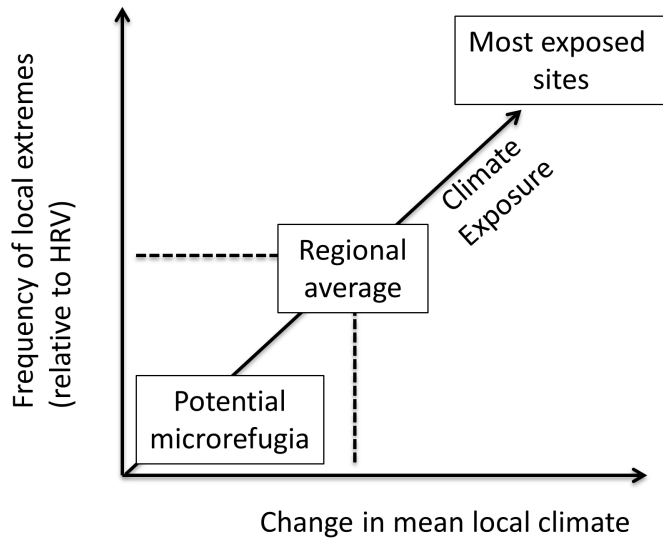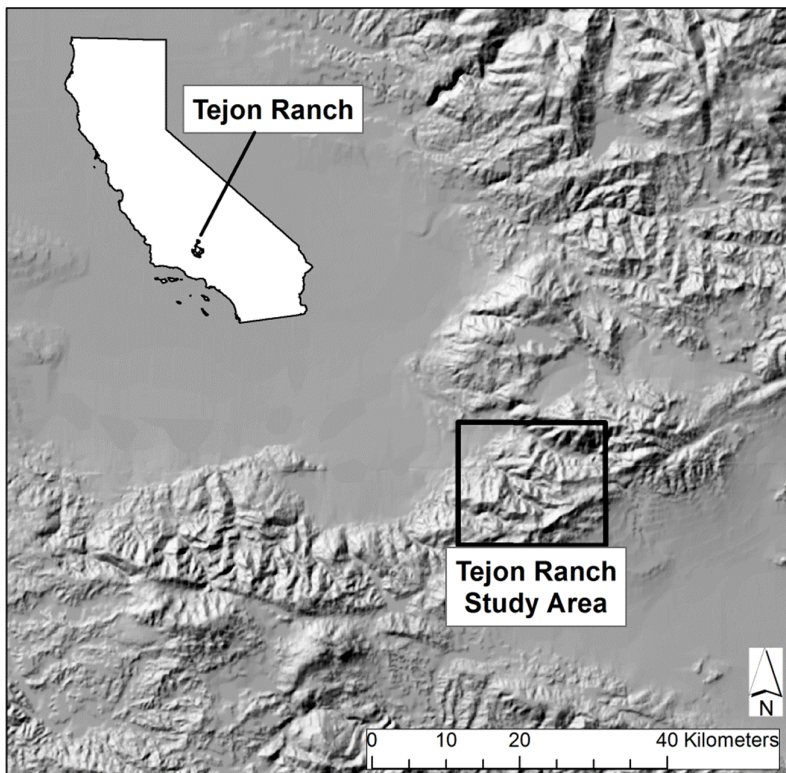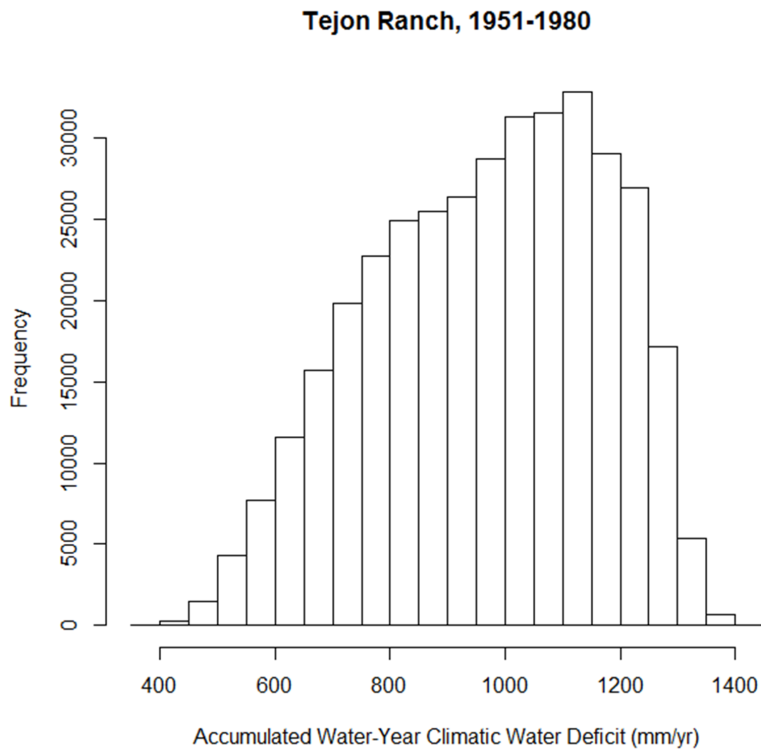
Fig. 1

Fig. 2

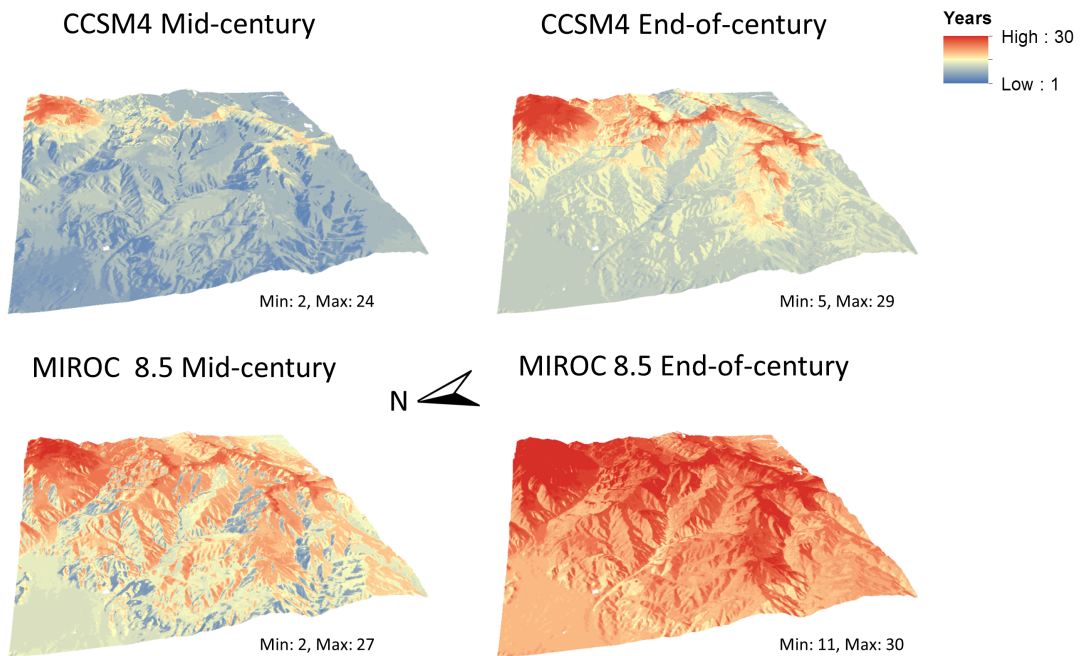Tejon Ranch, 1951-1980

670

Fig. 3

CCSM4 Mid-century   CCSM4 End-of-century

Years
High : 30
Low : 1

Min: 2, Max: 24   Min: 5, Max: 29

MIROC 8.5 Mid-century   MIROC 8.5 End-of-century

N

Min: 2, Max: 27   Min: 11, Max: 30

Fig. 4

Fig. 5

Fig. 6